

# $\kappa$ opioids selectively control dopaminergic neurons projecting to the prefrontal cortex

Elyssa B. Margolis<sup>\*†</sup>, Hagar Lock<sup>\*</sup>, Vladimir I. Chefer<sup>‡</sup>, Toni S. Shippenberg<sup>‡</sup>, Gregory O. Hjelmstad<sup>\*§</sup>, and Howard L. Fields<sup>\*§</sup>

<sup>\*</sup>Ernest Gallo Clinic and Research Center, University of California at San Francisco, Emeryville, CA 94608; <sup>‡</sup>Integrative Neuroscience Section, National Institute on Drug Abuse Intramural Research Program, National Institutes of Health, 5500 Nathan Shock Drive, Baltimore, MD 21224; and <sup>§</sup>Departments of Neurology and Physiology and The Wheeler Center for the Neurobiology of Addiction, University of California, San Francisco, CA 94143-0114

Communicated by Raymond L. White, University of California at San Francisco, Emeryville, CA, December 27, 2005 (received for review November 1, 2005)

Dopaminergic afferents arising from the ventral tegmental area (VTA) are crucial elements in the neural circuits that mediate arousal, motivation, and reinforcement. Two major targets of these afferents are the medial prefrontal cortex (mPFC) and the nucleus accumbens (NAc). Whereas dopamine (DA) in the mPFC has been implicated in working memory and attentional processes, DA in the NAc is required for responding to reward predictive cues. These distinct functions suggest a role for independent firing patterns of dopaminergic neurons projecting to these brain regions. In fact, DA release in mPFC and NAc can be differentially modulated. However, to date, electrophysiological studies have largely overlooked heterogeneity among VTA neurons. Here, we provide direct evidence for differential neurotransmitter control of DA neural activity and corresponding DA release based on projection target.  $\kappa$  opioid receptor agonists inhibit VTA DA neurons that project to the mPFC but not those that project to the NAc. Moreover, DA levels in the mPFC, but not the NAc, are reduced after local infusion of  $\kappa$  opioid receptor agonists into the VTA. These findings demonstrate that DA release in specific brain regions can be independently regulated by opioid targeting of a subpopulation of VTA DA neurons. Selective control of VTA DA neurons projecting to the mPFC has important implications for understanding addiction, attention disorders, and schizophrenia, all of which are associated with DA dysfunction in the mPFC.

GABA | reward | motivation | nucleus accumbens | ventral tegmental area

The dopaminergic neurons of the ventral tegmental area (VTA) play a critical role in motivation and reinforcement (1–3). Two major projection targets of VTA dopamine (DA) neurons are the medial prefrontal cortex (mPFC) and the nucleus accumbens (NAc). DA plays different roles in these two projection targets, contributing to working memory processes in the mPFC (4, 5) and motivated responding in the NAc (6). Despite evidence that DA levels in the mPFC and NAc are differentially modulated during various behavioral conditions (7, 8), electrophysiological studies have focused on the functional similarities among the VTA neurons.

The VTA is an important site for opioid control of goal-directed behaviors (9). We previously showed that  $\kappa$  opioid receptor (KOP-R) agonists directly inhibit a subset of DA neurons in the VTA through activation of a G-protein-coupled, inwardly rectifying potassium channel (10). This finding, in conjunction with previous reports that limbic and cortical projections arise from largely separate populations of VTA neurons (11, 12), led us to hypothesize that postsynaptic KOP-R agonist effects on VTA neurons segregate on the basis of projection target. To address this question, we made whole-cell, patch-clamp recordings in VTA neurons that were retrogradely labeled from the NAc or the mPFC and tested their postsynaptic sensitivity to KOP-R agonists. Neurons were filled with biocytin, and, after recording, brain slices were fixed and immunohistochemically processed for tyrosine hydroxylase (TH), a marker of dopaminergic neurons. To determine the *in vivo* relevance of

these results to DA release in the projection targets in question, we measured DA levels by microdialysis in the NAc and mPFC of awake, unrestrained rats after local delivery of a KOP-R agonist into the VTA.

## Results

DiI injections into the mPFC or NAc (Fig. 1 *A* and *B*) labeled cell bodies in the VTA and substantia nigra pars compacta (Fig. 1 *CI–C3*). To compare the density of these projections, retrogradely labeled neurons were counted in six regions of interest per slice (two fields in the lateral and one in the medial VTA, ipsilateral and contralateral to the unilateral injection site;  $\times 250$  magnification) in four nonadjacent horizontal 50- $\mu$ m slices per animal throughout the dorsoventral extent of the VTA. Approximately twice as many retrogradely labeled neurons were observed in the VTA after unilateral injections into the NAc ( $210 \pm 30$  neurons per animal,  $n = 4$ ) compared with unilateral mPFC injections ( $110 \pm 10$  neurons per animal,  $n = 6$ ). Coinjections of DiI into the NAc and FluoroGold into the mPFC of the same animal showed that a relatively small proportion of neurons expressed both markers ( $14 \pm 2$  double-labeled neurons per animal,  $n = 3$ ) (Fig. 1*D*): 19% of mPFC projections and 13% of NAc projections were colabeled. However, despite their distinct projections, the distributions of mPFC- and NAc-projecting neurons within the VTA were similar. These data from young rats are consistent with previous observations of smaller injection volumes in adult rats (11, 12), and the data support the hypothesis that largely separate populations of VTA neurons project to the mPFC and the NAc.

To compare the neurotransmitter content of these two projections, brain slices containing retrogradely labeled cells were immunohistochemically analyzed by using antibodies for TH and the 67-kDa form of glutamic acid decarboxylase (GAD67) (13), for identification of DA and GABA neurons, respectively. The mPFC and NAc projections each included TH(+) and GAD67(+) neurons (Fig. 2*A*). TH(+) neurons comprised  $45\% \pm 10\%$  ( $n = 6$  rats) of the mPFC and  $66\% \pm 10\%$  ( $n = 3$  rats) of NAc projections and were intermixed with TH(–) projections throughout the VTA (Fig. 2*B*). Similar percentages of GAD67(+) neurons were found among projections to the mPFC ( $20 \pm 6\%$ ,  $n = 7$  rats) and NAc ( $25 \pm 5\%$ ,  $n = 4$  rats) (Fig. 2*B*). That GAD67 and TH staining did not account for 100% of the retrogradely labeled neurons raises the possibility that some VTA projection neurons contain an alternative neurotransmitter, such as glutamate (14). However, it is also plausible that this

Conflict of interest statement: No conflicts declared.

Abbreviations: AP, anteroposterior; DA, dopamine; GAD67, 67-kDa glutamic acid decarboxylase; KOP-R,  $\kappa$  opioid receptor; mPFC, medial prefrontal cortex; ML, mediolateral; NAc, nucleus accumbens; nor-BNI, nor-binaltorphimine; TH, tyrosine hydroxylase; V, ventral; VTA, ventral tegmental area.

<sup>†</sup>To whom correspondence should be addressed at: Ernest Gallo Clinic and Research Center, 5858 Horton Street, Suite 200, Emeryville, CA 94608. E-mail: elyssam@egcrcr.net.

© 2006 by The National Academy of Sciences of the USA

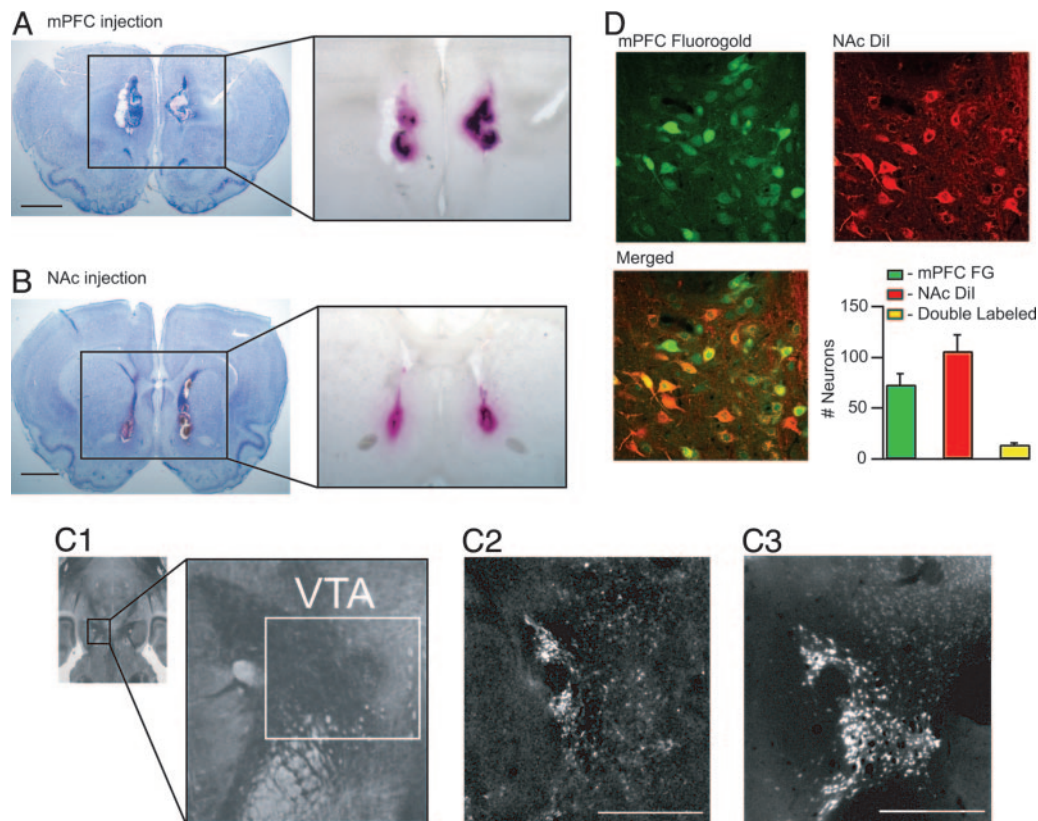


**Fig. 1.** VTA projections to the mPFC and NAc arise from different populations of neurons. (A and B) Sample coronal brain sections showing injection tracks (Left) and tracer deposits (Right) resulting from the bilateral injection of the retrograde tracer Dil into the mPFC (A) or the NAc (B). (Scale bars: 2 mm.) (C1) Horizontal brain slice. The white box in the magnified midbrain region identifies the VTA region where experiments were completed (modified from ref. 36). (C2 and C3) Sample horizontal slices of midbrain region showing transported Dil (white) 7 days after mPFC (C2) or NAc (C3) injections. (Scale bars: 1 mm.) (D) VTA section from a rat injected with FluoroGold (green) into the mPFC and Dil (red) into the NAc shows a minority of colabeled (yellow) neurons. Neurons examined throughout the VTA show a relatively small amount of colabeling in this protocol ( $n = 3$  rats).

difference in labeling represents an underestimation of GABAergic projections due to false negative results for GAD67 staining.

Stable whole-cell recordings were made in 50 retrogradely labeled neurons, of which both mPFC-projecting and NAc-

projecting were similarly scattered throughout the medial-lateral, anterior-posterior, and dorsal-ventral aspects of the VTA (see Fig. 5, which is published as supporting information on the PNAS web site). Of these recordings, 26 cells were recovered and subsequently processed for TH immunoreactivity. Among recovered mPFC projections, 10 of 17 neurons (59%) were TH(+). Seven of nine (78%) NAc-projecting neurons were TH(+).

We examined the electrophysiological properties of mPFC- and NAc-projecting neurons. DA neurons express a hyperpolarization-activated nonspecific cation current,  $I_h$ . Functionally,  $I_h$  generally contributes to pacemaker-like neuronal activity (15), although it is not clear whether this is the case in the VTA (16, 17). When randomly sampled, approximately two-thirds of  $I_h(+)$  VTA neurons are dopaminergic (10, 18). An  $I_h$  was detected in 95% (20 of 21) of NAc-projecting VTA neurons, but in only 62% (18 of 29) of mPFC-projecting neurons ( $P < 0.01$ , Fisher Exact test) (Fig. 3).  $I_h(-)$ , mPFC-projecting neurons were confirmed as TH(-) ( $n = 5$ ) (Fig. 3C). These neurons not only lacked an  $I_h$  but had other electrophysiological properties consistent with their classification as VTA secondary neurons (Table 1). Although secondary neurons have been proposed to be GABAergic interneurons (19), our data clearly demonstrate that many are projection neurons. Among  $I_h(+)$  neurons, those projecting to the mPFC expressed a significantly larger  $I_h$  than NAc projections (Fig. 3D). This difference was also present in confirmed TH(+) projections (Fig. 3E). Interestingly, the average action potential duration was the same for  $I_h(-)$  neurons and confirmed TH(+), mPFC-projecting neurons and was shorter

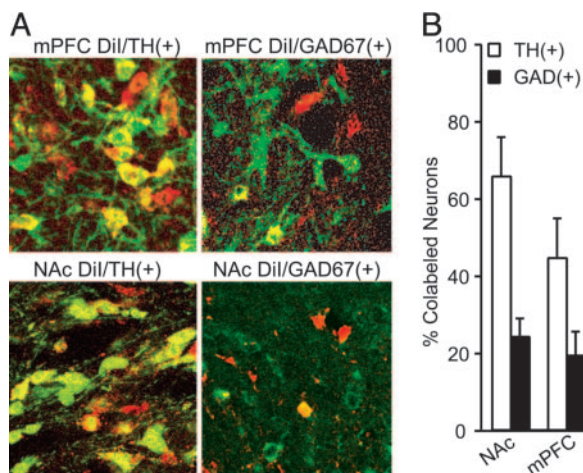


**Fig. 2.** Dopaminergic and GABAergic VTA neurons project to the mPFC and NAc. (A) VTA slices containing retrogradely labeled neurons (red) were immunohistochemically processed for TH or GAD67 immunoreactivity (green), and colabeling (yellow) was observed. (B) Quantified colabeling across animals (Nac/TH,  $n = 3$ ; Nac/GAD67,  $n = 4$ ; mPFC/TH,  $n = 6$ ; mPFC/GAD67,  $n = 7$ ).

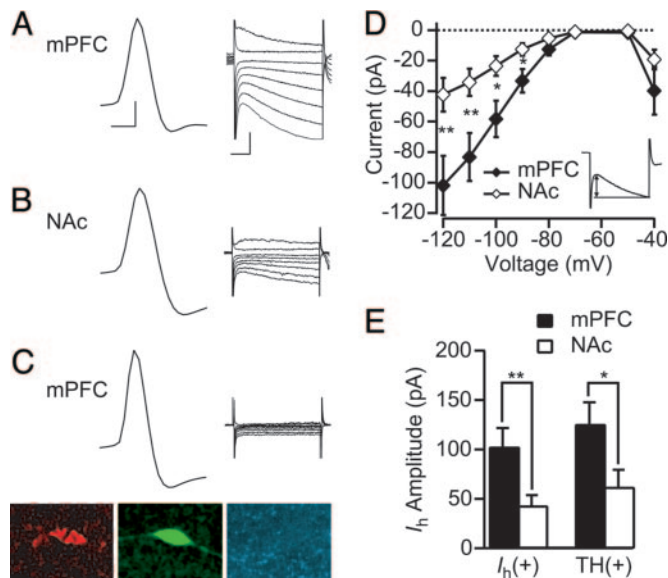


**Fig. 3.** VTA neurons with a larger  $I_h$  project to the mPFC. (A and B) Sample action potentials (calibration: 20 mV and 1 ms) and  $I_h$  curves (calibration: 100 pA and 50 ms) measured in mPFC-projecting (A) and NAc-projecting (B) VTA neurons. (C) Sample mPFC-projecting neuron lacking an  $I_h$ . This neuron was retrogradely labeled by Dil injection into the mPFC (red), filled with biocytin during recording (green), and was TH(-) (blue). (D) Among  $I_h(+)$  neurons, the  $I_h$  activated by a voltage step from  $-60$  mV to  $-90$ ,  $-100$ ,  $-110$ , and  $-120$  mV was significantly larger in mPFC projections ( $n = 18$ ) than in NAc projections ( $n = 20$ ). (Inset)  $I_h$  was measured as the difference between the initial and final current during a 200-ms voltage step. (E)  $I_h$  activation during a voltage step to  $-120$  mV was significantly larger in confirmed TH(+), mPFC-projecting neurons ( $n = 10$ ) than in NAc-projecting, TH(+), neurons ( $n = 7$ ). \*,  $P < 0.05$ ; \*\*,  $P < 0.01$ .

than the action potential durations of NAc-projecting neurons ( $P < 0.05$ ) (Table 1). For both projections, the action potential durations of  $I_h(+)$ , TH(-) projections were overlapping with those of the TH(+) neurons projecting to the same target region (data not shown). Initial membrane potential and action potential height were similar among mPFC- and NAc-projecting dopaminergic neurons (Table 1).

Twelve mPFC-projecting  $I_h(+)$  neurons were tested for a postsynaptic response to the KOP-R-selective agonist U69593 (*trans*-3,4-dichloro-*N*-methyl-*N*-[2-(1-pyrrolidinyl)-cyclohexyl] benzeneacetamide methane-sulfonate hydrate) at  $1 \mu\text{M}$ . Of these neurons, 83% (10 of 12) were significantly inhibited by U69593 [mean effect for all spontaneously firing neurons,  $50\% \pm 10\%$  inhibition of firing ( $n = 7$ ); for all quiescent neurons,  $4 \pm 2$  mV of hyperpolarization ( $n = 5$ )]. Of the KOP-R-agonist-tested neurons, 11 were recovered and processed for TH immunoreactivity. All of the mPFC-projecting confirmed TH(+) neurons (seven of seven) were inhibited by U69593 (Fig. 4A–C). Consistent with our previous finding that only dopaminergic neurons in the VTA are inhibited by KOP-R agonists (10), none

of the TH(-), mPFC-projecting neurons were inhibited by U69593 ( $n = 4$ ).

In contrast to mPFC projections, VTA neurons projecting to the NAc were not inhibited by U69593. Fifteen of 16 NAc-projecting  $I_h(+)$  neurons tested for a postsynaptic response to U69593 were unaffected. The mean change from baseline for all 16 neurons was also not significant [spontaneously firing neurons,  $6 \pm 6\%$  inhibition of firing ( $n = 3$ ); quiescent neurons,  $0.7 \pm 0.8$  mV of hyperpolarization ( $n = 13$ )]. Furthermore, none of the NAc-projecting VTA neurons histochemically identified as dopaminergic were inhibited by U69593 ( $n = 4$ ) (Fig. 4D–F).

To test the relevance of these findings to DA release *in vivo*, we used dual probe microdialysis to detect changes in DA levels in the mPFC or NAc of habituated, freely moving adult rats during reverse microdialysis delivery of U69593 ( $5 \mu\text{M}$ ) into the VTA. U69593 significantly decreased DA levels in the mPFC [ $n = 7$ ;  $F(1,6) = 13.3$ ;  $P < 0.05$ ] (Fig. 4G). This effect was blocked by intra-VTA perfusion of the KOP-R-selective antagonist nor-binaltorphimine (nor-BNI,  $1 \mu\text{M}$ ) before administration of U69593 ( $n = 3$ ) (Fig. 4G). Consistent with the electrophysiology, no changes in DA levels were observed in the NAc when U69593 was dialyzed into the VTA [ $n = 7$ ;  $F(1,6) = 0.193$ ;  $P > 0.05$ ] (Fig. 4H).

## Discussion

These data show that KOP-R agonists inhibit VTA DA neurons that project to the mPFC but not those projecting to the NAc. Despite the fact that separate subsets of midbrain DA neurons have distinct projection targets (11, 12, 20), the population as a whole is often considered to be physiologically and pharmacologically homogeneous. In addition to the pharmacological difference between these two subpopulations of DA projection neurons, we also show that the magnitude of one characteristic electrophysiological property of DA neurons,  $I_h$ , is correlated with projection target.

In this study, we identified two types of non-DA VTA projection neurons. Almost half of the mPFC-projecting neurons recorded in this study were  $I_h(-)$ , a characteristic of VTA secondary neurons, which previously were hypothesized to be GABAergic interneurons (19). There were also  $I_h(+)$  but TH(-) neurons projecting to both mPFC and NAc. The electrophysiological characteristics of these  $I_h(+)$  neurons were overlapping with those of the TH(+) neurons. Furthermore, three of four of the  $I_h(+)$ , TH(-) neurons recorded in this study had action potentials with longer durations than the recently suggested 1.1-msec criterion for dopaminergic neurons (21), and these durations overlapped with those of the TH(+) neurons reported here. Therefore, immunohistochemistry was the only consistently reliable method for identifying the subset of  $I_h(+)$  neurons that were dopaminergic.

By demonstrating a clear pharmacological difference between subgroups of VTA DA neurons based on projection target, our experiments demonstrate that subsets of VTA DA neurons can be independently modulated and suggest that they participate in distinct circuits. One such DA circuit could include VTA-projecting neurons from the lateral hypothalamus or NAc that

**Table 1.** Electrophysiological properties of VTA projection neurons

Neurons	$I_h$	TH	Initial membrane potential, mV	Action potential height, mV	Action potential width, ms	$n$
mPFC-projecting	-	-	$-47 \pm 3$	$97 \pm 7$	$1.1 \pm 0.2$	11*
	+	+	$-42 \pm 3$	$89 \pm 5$	$1.1 \pm 0.1$	10
NAc-projecting	+	+	$-44 \pm 1$	$80 \pm 10$	$1.5 \pm 0.3$	7

\*The five  $I_h(-)$ , mPFC-projecting neurons processed for TH were confirmed to be TH(-). Therefore, all 11  $I_h(-)$ , mPFC-projecting neurons were pooled here.

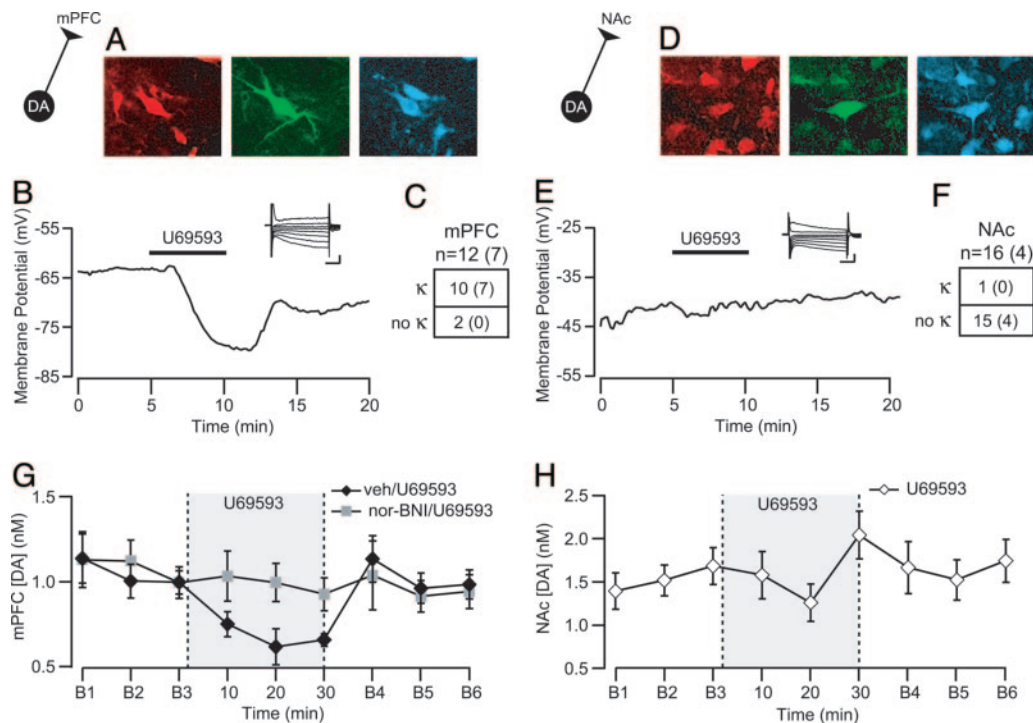


**Fig. 4.** DA neurons that project to the mPFC but not to the NAc are inhibited by KOP-R agonists. (A) Example of a neuron labeled with Dil after injection into the mPFC (red), filled with biocytin during recording (green), and immunohistochemically confirmed as TH(+) (blue). (B) This neuron expressed a prominent  $I_h$  (inset; scale bar: 100 pA and 50 ms) and was inhibited by the KOP-R agonist U69593 (1  $\mu$ M). (C) Summary of U69593 effects in mPFC-projecting  $I_h$ (+) neurons. The numbers of confirmed TH(+) neurons are in parentheses. (D) Example neuron labeled with Dil after injection into the NAc (red), filled with biocytin during recording (green), and immunohistochemically confirmed as TH(+) (blue). (E) This neuron expressed an  $I_h$  (inset; calibration: 100 pA and 50 ms) and was unaffected by U69593 (1  $\mu$ M). (F) U69593 inhibited only one NAc-projecting  $I_h$ (+) neuron. The numbers of confirmed TH(+) neurons are in parentheses. (G) *In vivo* measurement of DA in the mPFC using microdialysis shows that perfusion of 5  $\mu$ M U69593 into the VTA significantly decreased mPFC DA levels ( $n = 7$ ). This effect was blocked by administration of the KOP-R-selective antagonist nor-BNI at 1  $\mu$ M ( $n = 3$ ). (H) Intra-VTA U69593 did not change DA levels in the NAc ( $n = 6$ ).

contain the KOP-R-selective endogenous peptide dynorphin (DYN) (22, 23). DYN terminals synapse onto DA dendrites in the VTA (24) and are therefore optimally positioned to control DA neuron signaling by a direct postsynaptic action. The fact that DYN levels in the midbrain increase after amphetamine administration (25) suggests that KOP-R-mediated control of midbrain DA neurons projecting to the mPFC can have powerful behavioral effects. Furthermore, administration of drugs of abuse, such as alcohol and cocaine, produce long-lasting down-regulation of KOP-R mRNA levels in the VTA (26). The resulting changes in KOP-R expression may play an important role in the prolonged changes in mPFC DA signaling and behavior that are induced by exposure to these drugs (27–29).

The dissociation between mPFC and NAc DA functioning is underscored by models of many cognitive disorders, including schizophrenia (30) and attention deficit hyperactivity disorder (31), characterized by DA dysfunction specifically in the mPFC. DA signaling in the mPFC, but not the NAc, has also been implicated in animal models of cocaine relapse (32). Alterations in DA release in the cortex may also contribute to the psychotomimetic effects of KOP-R activation in humans (33). Thus, mechanisms of differential modulation of dopaminergic afferents to the mPFC offer an important avenue for understanding and treating these common disorders.

## Materials and Methods

**Anatomy and Electrophysiology. Retrograde tracer injections.** All retrograde-labeling experiments conformed to National Institutes of Health and Ernest Gallo Clinic and Research Center animal care policy standards. Male, 27-day-old Sprague–Dawley rats (Harlan Laboratories, San Diego) were anesthetized with isoflu-

rane. A 1- $\mu$ l Hamilton syringe was stereotaxically placed in either the mPFC [anteroposterior (AP), +2.6 mm from bregma; mediolateral (ML),  $\pm$ 0.8 mm from bregma; ventral (V), –4.0 mm from skull surface] or the NAc (AP, +1.5; ML,  $\pm$ 0.8; V, –6.7). Neuro-Dil (1  $\mu$ l, 7% in ethanol; Biotium, Hayward, CA) or hydroxystilamide (FluoroGold 3% in H<sub>2</sub>O; Biotium) was slowly injected. Bilateral and unilateral injections were performed for electrophysiological and anatomical studies, respectively. Coronal sections containing mPFC or NAc were prepared with a sliding microtome and stained with 0.2% thionin to confirm all injection placements.

Standard methods were used for immunohistochemistry (see *Supporting Materials and Methods*, which is published as supporting information on the PNAS web site).

**Slice preparation and electrophysiology.** All recordings were made blind to injection site. Experiments were carried out 6–8 days after injection. Slice preparation, electrophysiological recordings, and data analysis were completed as described in ref. 10. Horizontal brain slices (150  $\mu$ m thick) were prepared by using a vibratome (Leica Instruments, Solm, Germany) in Ringer solution (119 mM NaCl/2.5 mM KCl/1.3 mM MgSO<sub>4</sub>/1.0 mM NaH<sub>2</sub>PO<sub>4</sub>/2.5 mM CaCl<sub>2</sub>/26.2 mM NaHCO<sub>3</sub>/11 mM glucose saturated with 95% O<sub>2</sub>/5% CO<sub>2</sub>). Slices were visualized under a Zeiss Axioskop with differential interference contrast optics and infrared and epifluorescent illumination to visualize projecting neurons during recording.

Whole-cell recordings were made at 33°C with 2.5–4 M $\Omega$  pipettes containing 123 mM K-gluconate, 10 mM Hepes, 0.2 mM EGTA, 8 mM NaCl, 2 mM MgATP, 0.3 mM Na<sub>3</sub>GTP, and 0.1% biocytin (pH 7.2, osmolarity adjusted to 275). Pharmacological

experiments were carried out in current clamp mode ( $I = 0$ ), measuring instantaneous firing rate and/or membrane potential.

U69593 was applied by bath superfusion. U69593 stock solution (1 mM diluted in 50% EtOH) was diluted in Ringer solution immediately before application. Drugs were obtained from Sigma.

**Data analysis.**  $I_h$  was recorded by voltage clamping cells at  $-60$  mV and stepping to  $-40$ ,  $-50$ ,  $-70$ ,  $-80$ ,  $-90$ ,  $-100$ ,  $-110$ , and  $-120$  mV.  $I_h$  magnitude was measured as the difference between the initial capacitive response to the voltage step and the final step current.

Differences between NAc and mPFC projection populations were tested with a one-way ANOVA. The action potential width was taken as the width at half the height of the action potential. The action potential height was measured as the potential difference between the peak of the spike and the immediately following trough.  $P < 0.05$  was required for significance in all analyses.

**Microdialysis. Animals.** Male, 250- to 300-g Sprague–Dawley rats (Charles River Laboratories) were housed in facilities accredited by the American Association for the Accreditation of Laboratory Animal Care, and experiments were reviewed by the National Institute on Drug Abuse Intramural Research Program Institutional Care and Use Committee under National Institute on Drug Abuse (National Institutes of Health) guidelines.

**Surgical procedures.** Standard stereotaxic procedures were used to implant two unilateral microdialysis guide cannulae (CMA/11; CMA/Microdialysis, Acton, MA) in the NAc and VTA or mPFC and VTA (NAc: AP,  $+1.6$  mm from bregma; ML,  $\pm 0.9$  mm from bregma; V,  $-6.0$  mm from dura surface; mPFC: AP,  $+3.2$  mm from bregma; ML,  $\pm 0.6$  mm from bregma; V,  $-2.0$  mm from dura surface; VTA: AP,  $-5.6$  mm from bregma; ML,  $\pm 0.6$  mm from bregma; V,  $-7.5$  mm from dura surface) of animals anesthetized i.p. with 3 ml/kg Equithesin.

**Microdialysis procedures.** Microdialysis experiments, as described in ref. 34, commenced 5 days after surgery. Before measurements, each probe was flushed overnight with  $0.3 \mu\text{l}/\text{min}$  artificial cerebrospinal fluid (aCSF) containing 145 mM NaCl, 2.8 mM KCl, 1.2 mM  $\text{MgCl}_2$ , 1.2 mM  $\text{CaCl}_2$ , 0.25 mM ascorbic acid, and 5.4 mM D-glucose, adjusted to pH 7.2 with HPLC-grade NaOH or  $\text{H}_3\text{PO}_4$ . During the experiment, fresh aCSF was perfused at

$0.6 \mu\text{l}/\text{min}$ . After 60 min of equilibration, 10-min dialysate sample collection commenced. All drugs were administered into the VTA by reverse dialysis. After baseline determination, the VTA aCSF was changed to that containing  $5 \mu\text{M}$  U69593, and, after 30 min of equilibration, three consecutive samples were collected. To confirm receptor selectivity, experiments were conducted in a parallel group of rats that received the selective KOP-R antagonist nor-BNI at  $1 \mu\text{M}$  perfused for 30 min before other drugs ( $n = 3$ ) via the VTA dialysis probe (35).

**Probe location confirmation.** Upon completion of all experiments, the GABA<sub>B</sub> receptor agonist baclofen ( $50 \mu\text{M}$ ) was added to the VTA artificial cerebrospinal fluid to inactivate neurons and therefore pharmacologically confirm a functional connection between DA neurons targeted by the VTA probe and the projection target probe and to demonstrate that the dialysis method was sensitive to changes in DA concentration due to VTA neuron inhibition. Baclofen significantly reduced basal mPFC DA levels in saline-treated animals and nor-BNI-treated animals (decrease from baseline for saline:  $0.52 \pm 0.09$  nM,  $n = 7$ ; nor-BNI:  $0.9 \pm 0.6$  nM,  $n = 3$ ) and in the NAc (decrease from baseline:  $0.6 \pm 0.2$  nM).

For anatomical confirmation, animals were euthanized by Equithesin, and probe placement was assessed on  $25\text{-}\mu\text{m}$ , serial coronal cryostat sections. Only data obtained from animals with histologically correct placements were used for subsequent analysis.

**DA determination.** DA was determined by HPLC coupled to electrochemical detection as described in ref. 34. The retention time for DA was 2.5 min, and the limit of detection was  $<0.25$  nM.

**Data analysis.** Drug effects were analyzed by repeated-measures ANOVA, with one between-subjects factor (brain region) and two within-subjects factors (drug challenge and time). The data are presented as mean  $\pm$  SEM. The accepted value of significance was  $P < 0.05$ .

This work was supported by Department of the Army Award DAMD17-03-1-0059, National Institute on Drug Abuse Award DA-15686, and Integrative Neuroscience Initiative on Alcoholism Project Award AA U01 13486 from the National Institute on Alcohol Abuse and Alcoholism and by the National Institute on Drug Abuse Intramural Research Program and the State of California for medical research on alcohol and substance abuse through the University of California, San Francisco.

- McClure, S. M., Daw, N. D. & Montague, P. R. (2003) *Trends Neurosci.* **26**, 423–428.
- Schultz, W. (2002) *Neuron* **36**, 241–263.
- Wise, R. A. (2004) *Nat. Rev. Neurosci.* **5**, 483–494.
- Williams, G. V. & Goldman-Rakic, P. S. (1995) *Nature* **376**, 572–575.
- Chudasama, Y. & Robbins, T. W. (2004) *Psychopharmacology* **174**, 86–98.
- Yun, I. A., Wakabayashi, K. T., Fields, H. L. & Nicola, S. M. (2004) *J. Neurosci.* **24**, 2923–2933.
- Di Chiara, G., Loddo, P. & Tanda, G. (1999) *Biol. Psychiatry* **46**, 1624–1633.
- Bassareo, V. & Di Chiara, G. (1997) *J. Neurosci.* **17**, 851–861.
- Bals-Kubik, R., Ableitner, A., Herz, A. & Shippenberg, T. S. (1993) *J. Pharmacol. Exp. Ther.* **264**, 489–495.
- Margolis, E. B., Hjelmstad, G. O., Bonci, A. & Fields, H. L. (2003) *J. Neurosci.* **23**, 9981–9986.
- Swanson, L. W. (1982) *Brain Res. Bull.* **9**, 321–353.
- Fallon, J. H. (1981) *J. Neurosci.* **1**, 1361–1368.
- Kaufman, D. L., Houser, C. R. & Tobin, A. J. (1991) *J. Neurochem.* **56**, 720–723.
- Chuhma, N., Zhang, H., Masson, J., Zhuang, X., Sulzer, D., Hen, R. & Rayport, S. (2004) *J. Neurosci.* **24**, 972–981.
- Luthi, A. & McCormick, D. A. (1998) *Neuron* **21**, 9–12.
- Appel, S. B., Liu, Z., McElvain, M. A. & Brodie, M. S. (2003) *J. Pharmacol. Exp. Ther.* **306**, 437–446.
- Neuhoff, H., Neu, A., Liss, B. & Roeper, J. (2002) *J. Neurosci.* **22**, 1290–1302.
- Jones, S. & Kauer, J. A. (1999) *J. Neurosci.* **19**, 9780–9787.
- Johnson, S. W. & North, R. A. (1992) *J. Neurosci.* **12**, 483–488.
- Carr, D. B. & Sesack, S. R. (2000) *J. Neurosci.* **20**, 3864–3873.
- Ungless, M. A., Magill, P. J. & Bolam, J. P. (2004) *Science* **303**, 2040–2042.
- Fallon, J. H., Leslie, F. M. & Cone, R. I. (1985) *Neuropeptides* **5**, 457–460.
- Meredith, G. E. (1999) *Ann. N.Y. Acad. Sci.* **877**, 140–156.
- Pickel, V. M., Chan, J. & Sesack, S. R. (1993) *Brain Res.* **602**, 275–289.
- Bustamante, D., You, Z. B., Castel, M. N., Johansson, S., Gojny, M., Terenius, L., Hofkelt, T. & Herrera-Marschitz, M. (2002) *J. Neurochem.* **83**, 645–654.
- Rosin, A., Lindholm, S., Franck, J. & Georgieva, J. (1999) *Neurosci. Lett.* **275**, 1–4.
- Wu, W. R., Li, N. & Sorg, B. A. (2003) *Brain Res.* **991**, 232–239.
- Horger, B. A., Valadez, A., Wellman, P. J. & Schenk, S. (1994) *Life Sci.* **55**, 1245–1251.
- Sorg, B. A., Davidson, D. L., Kalivas, P. W. & Prasad, B. M. (1997) *J. Pharmacol. Exp. Ther.* **281**, 54–61.
- Yang, C. R., Seamans, J. K. & Gorelova, N. (1999) *Neuropsychopharmacology* **21**, 161–194.
- Viggiano, D., Vallone, D., Ruocco, L. A. & Sadile, A. G. (2003) *Neurosci. Biobehav. Rev.* **27**, 683–689.
- McFarland, K. & Kalivas, P. W. (2001) *J. Neurosci.* **21**, 8655–8663.
- Pfeiffer, A., Brantl, V., Herz, A. & Emrich, H. M. (1986) *Science* **233**, 774–776.
- Chefer, V. I., Czyzyk, T., Bolan, E. A., Moron, J., Pintar, J. E. & Shippenberg, T. S. (2005) *J. Neurosci.* **25**, 5029–5037.
- Spanagel, R., Herz, A. & Shippenberg, T. S. (1992) *Proc. Natl. Acad. Sci. USA* **89**, 2046–2050.
- Paxinos, G. & Watson, C. (1998) *The Rat Brain in Stereotaxic Coordinates* (Academic, San Diego).